GA–A25862

# RESISTIVE WALL MODE STABILIZATION IN SLOWLY ROTATING HIGH BETA PLASMAS


by

H. REIMERDES, A.M. GAROFALO, M. OKABAYASHI, E.J. STRAIT, R. BETTI, M.S. CHU, B. HU, Y. IN, G.L. JACKSON, R.J. LA HAYE, M.J. LANCTOT, Y.Q. LIU, G.A. NAVRATIL, W.M. SOLOMON, H TAKAHASHI, R.J. GROEBNER, and the DIII-D TEAM



JULY 2007

## DISCLAIMER

GA–A25862

# RESISTIVE WALL MODE STABILIZATION IN SLOWLY ROTATING HIGH BETA PLASMAS

by
H. REIMERDES,* A.M. GAROFALO,* M. OKABAYASHI,† E.J. STRAIT, R. BETTI,‡
M.S. CHU, B. HU,‡ Y. IN,¶ G.L. JACKSON, R.J. LA HAYE, M.J. LANCTOT,* Y.Q. LIU,§
G.A. NAVRATIL,* W.M. SOLOMON,† H TAKAHASHI,† R.J. GROEBNER,
and the DIII-D TEAM

This is a preprint of an invited paper to be presented at the 34th EPS Conf. on Plasma Physics, in Warsaw, Poland, July 2-7, 2007 and to be published in the *Proceedings.*

*Columbia University, New York, New York.
†Princeton Plasma Physics Laboratory, Princeton, New Jersey.
‡University of Rochester, Rochester, New York.
¶FAR-TECH, Inc., San Diego, California.
§Chalmers University of Technology, Göteborg, Sweden.

Work supported by
the U.S. Department of Energy
under DE-FG02-89ER53297, DE-AC02-76CH03073, and DE-FG02-03ER83657

GENERAL ATOMICS PROJECT 30200
JULY 2007

GENERAL ATOMICS

# Resistive wall mode stabilization in slowly rotating high beta plasmas

**H Reimerdes[1], A M Garofalo[1], M Okabayashi[2], E J Strait[3], R Betti[4], M S Chu[3], B Hu[4], Y In[5], G L Jackson[3], R J La Haye[3], M J Lanctot[1], Y Q Liu[6], G A Navratil[1], W M Solomon[2], H Takahashi[2], R J Groebner[3] and the DIII-D team**

[1] Columbia University, New York, New York 10027, USA
[2] Princeton Plasma Physics Laboratory, Princeton, New Jersey 08543-0451, USA
[3] General Atomics, San Diego, California 92186-5608, USA
[4] University of Rochester, Rochester, New York 14627, USA
[5] FAR-TECH, Inc., San Diego, California 92121, USA
[6] Chalmers University of Technology, S-412 96 Göteborg, Sweden

E-mail: `hr2012@columbia.edu`

**Abstract.** DIII-D experiments show that the resistive wall mode (RWM) can remain stable in high $\beta$ scenarios despite a low net torque from nearly balanced neutral beam injection (NBI) heating. The minimization of magnetic field asymmetries is essential for operation at the resulting low plasma rotation of less than 20 krad/s (measured with charge exchange recombination spectroscopy using C VI emission) corresponding to less than 1% of the Alfvén velocity or less than 10% of the ion thermal velocity. In the presence of $n$=1 field asymmetries the rotation required for stability is significantly higher and depends on the torque input and momentum confinement, which suggests that a loss of torque-balance can lead to an effective rotation threshold above the linear RWM stability threshold. Without an externally applied field the measured rotation can be too low to neglect the diamagnetic rotation. A comparison of the instability onset in plasmas rotating with and against the direction of the plasma current indicates the importance of the toroidal flow driven by the radial electric field in the stabilization process. Observed rotation thresholds are compared with predictions for the semi-kinetic damping model, which generally underestimates the rotation required for stability. A more detailed modeling of kinetic damping including diamagnetic and precession drift frequencies can lead to stability without plasma rotation. However, even with corrected error-fields and fast plasma rotation, plasma generated perturbations, such as edge localized modes, can nonlinearly destabilize the RWM. In these cases feedback control can increase the damping of the magnetic perturbation and is effective in extending the duration of high $\beta$ discharges.

## 1. Introduction

The stabilization of the resistive wall mode (RWM) is an integral part of the high pressure, fully noninductive advanced tokamak path towards a fusion reactor, and a prerequisite for any operational scenario in which the plasma pressure exceeds the ideal magnetohydrodynamic (MHD) no-wall kink stability limit [1]. The growth of the ideal MHD long-wavelength kink mode is slowed by resistive diffusion of the perturbed magnetic field through nearby conducting structures, such as the vacuum vessel wall. The growth time of this so-called RWM is on the order of the characteristic eddy current decay time of the wall, $\tau_{\mathrm{W}}$. After the RWM was first observed in a reversed-field pinch [2], tokamak experiments revealed that the toroidal plasma rotation generated by uni-directional neutral beam injection (NBI) heating, which is typically in the order of a few percent of the Alfvén velocity, is sufficient to stabilize the RWM [3, 4, 5]. Sustaining the plasma rotation was also essential in the demonstration of the ultimate potential of wall stabilization by operating in the vicinity of the ideal MHD limit assuming an ideally conducting wall [6]. In DIII-D this has allowed for roughly a doubling of the value of $\beta = 2\mu_0 \langle p \rangle / B^2$, which is the ratio of volume averaged plasma pressure and magnetic field pressure, over the no-wall limit. Experiments in various devices, which used non-axisymmetric magnetic fields to slow the NBI driven plasma rotation, suggested that RWM stability requires toroidal plasma rotation in the range from 0.5% to 5% of the Alfvén velocity, when evaluated at the $q$=2 surface [7, 8]. Recent experiments in the DIII-D [9] and JT-60U [10] tokamaks with nearly balanced NBI heating have revealed a significant reduction of the required rotation for RWM stabilization.

## 2. Reduced rotation threshold in axisymmetric configuration

The DIII-D tokamak, equipped with up to 10 MW of balanced NBI heating power, can access high values of $\beta$ with a low net torque input. In discharge 126496 the plasma pressure is raised above the no-wall limit, figure 1(a), which in this "weakly" shaped lower single-null discharge with monotonic or slightly reversed central safety factor profile and $1 < q_{\min} < 2$, typically is $\beta_{N,\mathrm{nw}} \approx 2.5\ell_i$. At high $\beta$ the NBI torque $T_{\mathrm{NBI}}$ is reduced to 1.5 Nm, figure 1(b), which is approximately 20% of the torque uni-directional NBI heating would apply. Currents in non-axisymmetric coils are optimized to correct the $n$=1 component of the intrinsic error field. Stability is maintained while the toroidal rotation frequency $\Omega_\phi = V_\phi / R$ decreases to less than 20 krad/s across the entire profile, figure 1(c,d). Here the plasma rotation is measured with charge exchange recombination (CER) spectroscopy using C VI emission, which yields the toroidal and poloidal rotation velocity of carbon impurity ions. The toroidal rotation velocity corresponds to less than 1% of the inverse of the Alfvén time $\tau_{\mathrm{A}} = R_0(\mu_0\rho)^{1/2}/B_0$, where $R_0$ is the major radius, $B_0$ the toroidal magnetic field on axis and $\rho$ the local mass density, or less than 10% of the inverse of a characteristic ion thermal time $\tau_{i,\mathrm{th}} = R_0/(2k_{\mathrm{B}}T_i/m_i)^{1/2}$, where $T_i$ is the ion temperature and $m_i$ the ion mass.

Stable discharges are observed with plasma pressures up to 1.4 times the no-wall kink stability limit. Similar discharges at different values of $\beta$ show a low rotation threshold of $\Omega_\phi\, \tau_{\mathrm{A}}|_{q=2} \approx 0.003$, which is independent of $\beta$ [11]. The observed threshold values and its $\beta$ dependence are remarkably similar to the results obtained on JT-60U [10].

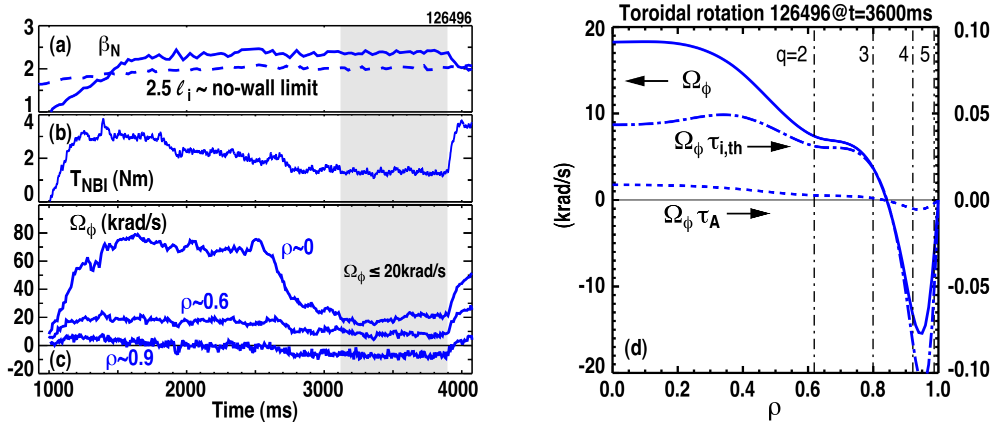


**Figure 1.** Beta is sustained above the no-wall stability limit (a) despite a decrease of the NBI torque $T_{\rm NBI}$ to a nearly balanced configuration (b). The toroidal rotation $\Omega_\phi$ decreases for ∼800 ms below 20 krad/s (c) across the entire profile (d). The rotation values correspond to less than 10% of the inverse of the ion thermal time $\tau_{\rm i,th}$ or less than 1% of the inverse of the Alfvén time $\tau_{\rm A}$ (d).

### *2.1. Comparison with rotation thresholds in the presence of a non-axisymmetric magnetic field*

The rotation threshold with nearly balanced NBI heating is, in particular, much lower than the threshold values found by applying non-axisymmetric magnetic fields to slow the plasma rotation. A comparison of discharge 118715 with uni-directional NBI heating, where an $n$=1 magnetic field is applied to slow the rotation, with the similar discharge 127941 with low NBI torque and good error field correction shows a decrease of the rotation threshold across the entire profile in the low-torque case, figure 2(a). Since the rotation profiles are not self-similar the reduction varies between a factor of 14 in the plasma center and little change near the edge.

A survey of the rotation threshold obtained by applying an $n$=1 magnetic field in various wall-stabilized scenarios reveals a dependence of the rotation threshold evaluated at the $q$=2 surface $V_{\rm crit}$ on the rotation before the braking is applied $V_0$ [12]. Variations in the NBI torque and the momentum confinement lead to a variation of $V_0$ over one order of magnitude. While the measured threshold $V_{\rm crit}$ also varies over an order of magnitude, the ratio of $V_{\rm crit}$ and $V_0$ remains in a narrow band between 1/3 and 2/3, figure 2(b). Such a behavior is hard to reconcile with a linear RWM stability threshold and suggests that the rotation collapse is caused by a loss of momentum balance. In a zero-dimensional model,

$$\frac{dV}{dt} = \frac{V_0 - V}{\tau_L} - \frac{1}{MR_0} T_{\rm MB} \quad , \qquad (1)$$

where $M$ is the mass of the plasma, a magnetic braking torque $T_{\rm MB}$, which is proportional to $V^{-1}$, would lead to a loss of momentum balance once the applied magnetic braking torque becomes large enough to decrease the plasma rotation below $V_{\rm crit} = 0.5\,V_0$, consistent with the experimental observation. Such a torque could be provided by an electro-magnetic torque as described by the induction motor model [12, 13]. A more complete description of the magnetic braking at high beta has to include the enhancement of the braking torque in the wall stabilized regime. Modeling

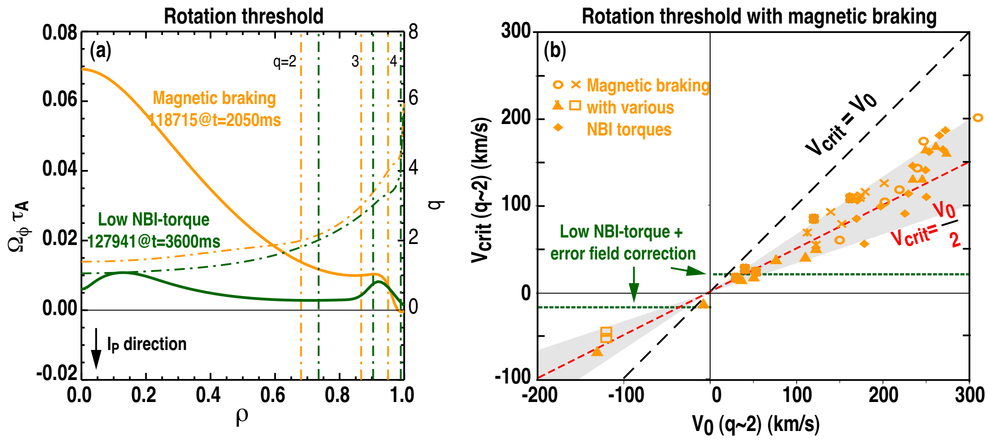


**Figure 2.** (a) The rotation threshold found with low NBI torque and good error field correction (127941) is lower than in a similar discharge with uni-directional NBI heating and $n$=1 magnetic braking (118715) across 95% of the profile. (b) The rotation threshold $V_{\rm crit}$ evaluated at the $q$=2 surface in discharges with quasi-static $n$=1 braking depends on the rotation $V_0$ before the braking field is applied. The dotted line indicates the rotation threshold observed without applying an $n$=1 field in the low NBI torque, lower single-null plasma.

of the plasma response and the resulting rotation evolution based on the Fitzpatrick-Aydemir RWM dispersion relation [14] leads to qualitatively similar behavior [11]. The increase of the effective RWM rotation threshold with applied $n$=1 fields implies a limit on tolerable error fields which supposedly can be traded off against an increased momentum input.

### *2.2. Rotation profile components*

The low rotation thresholds with optimized $n$=1 error field correction are too low to neglect the diamagnetic rotation $\omega_{\star {\rm i},j}=-(Z_j n_j e)^{-1} dP_j/d\psi$, where $P_j$ is the ion pressure, $Z_j$ the charge state, $\psi$ the poloidal flux per radian and $j$ denotes the ion species. This also implies a significant difference between the deuterium main ion rotation and the measured carbon impurity rotation. Assuming incompressibility, no radial flows and force balance, the rotation can be decomposed into two parts,

$$\vec{V}_j = k_j(\psi)\vec{B} + R\Omega_j(\psi)\vec{e}_\phi \quad , \tag{2}$$

where $k_j$ and $\Omega_j$ are flux functions. Equation (2) shows that $V_{\phi,j}/R$ is only a flux function if the poloidal rotation vanishes (i.e. if $k_j = 0$). In DIII-D, simultaneous measurements of $V_{\phi,{\rm C}}$ and $V_{\theta,{\rm C}}$ yield $k_{\rm C}$ and $\Omega_{\rm C}$ of carbon impurities. The radial force balance links the ion species via the radial electric field $E_r$,

$$\Omega_i = \frac{E_r}{RB_\theta} - (Z_i n_i e)^{-1}\frac{dP_i}{d\psi} \quad . \tag{3}$$

The toroidal rotation frequency can, therefore, be decomposed into the toroidal flow driven by the radial electric field, $\omega_E$=$E_r/(RB_\theta)$ and a diamagnetic component, $\Omega_j = \omega_E + \omega_{\star {\rm i},j}$. Since the CER diagnostic also measures the impurity pressure $P_{\rm C}$, $E_r$ can be calculated from equation (3). Assuming that deuterium and carbon ions have the same temperatures, electron density measurements using Thomson scattering lead

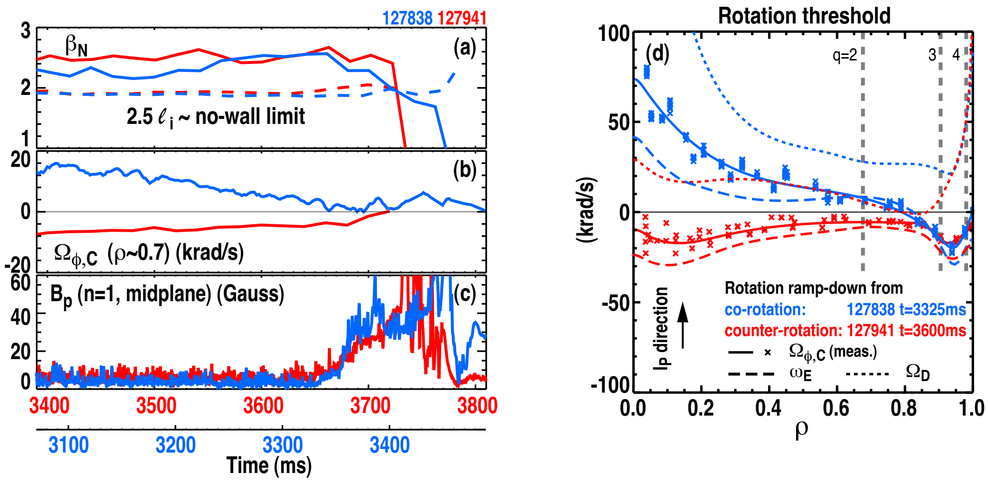


**Figure 3.** Comparison of NBI torque ramp down experiments in (a) two wall-stabilized discharges, which (b) differ in the direction of the rotation with respect to the plasma current: co-rotation in 127838 (blue), counter-rotation in 127941 (red). Both discharges lead to (c) a slowly growing $n$=1 RWM. (d) While the carbon rotation $\Omega_{\phi,\mathrm{C}}$ and $\omega_E$ profiles are of similar magnitude, the toroidal rotation frequencies of deuterium ions $\Omega_\mathrm{D}$ differ greatly across most (∼90%) of the profile.

to an estimate of $P_\mathrm{D}$, $\omega_{\star\mathrm{i,D}}$ and eventually $\Omega_\mathrm{D}$. The poloidal rotation for deuterium is predicted by neoclassical theory but its applicability is questionable [15].

In order to investigate the role of $\Omega_\mathrm{D}$ versus $\omega_E$, rotation thresholds in plasmas rotating in the direction of the plasma current (co-rotation) and against the direction of the plasma current (counter-rotation) are compared in otherwise similar plasmas, figure 3(a,b). In both discharges the rotation ramp-down leads to a slowly growing RWM, figure 3(c). The measured carbon rotation profiles $\Omega_{\phi,\mathrm{C}}$ at the mode onset have very different shapes, figure 3(d), with the rotation ramp-down from co-rotation leading to a profile, which changes its sign to counter-rotation near the plasma edge. The resulting $\omega_E$ profiles still have different shapes but their magnitudes are similar over large parts of the profile. In particular the magnitude of $\omega_E$ at all resonant surfaces agrees within 10%. This is in contrast to the derived $\Omega_\mathrm{D}$ profiles, which differ by more than a factor of 3 over 90% of the radius. Apart from the possibility of a rotation offset, the comparison of rotation threshold in co- and counter-rotation suggests the importance of $\omega_E$ for the stabilization process.

## 3. Active measurement of stable mode

The RWM stability is also investigated using active MHD spectroscopy, which yields a measurement of the growth rate $\gamma_\mathrm{RWM}$ and rotation frequency $\omega_\mathrm{RWM}$ of the mode, while the plasma is still stable [16]. In order to derive $\gamma_\mathrm{RWM}$ and $\omega_\mathrm{RWM}$ from a measurement at a single frequency, the coupling of the external coils to the RWM has to be determined from a measurement of the entire spectrum [12].

In discharge 125703, figure 4(a-c), an externally applied, low amplitude $n$=1 magnetic field rotates with 25 Hz in the direction of the plasma rotation, while $\beta$ and

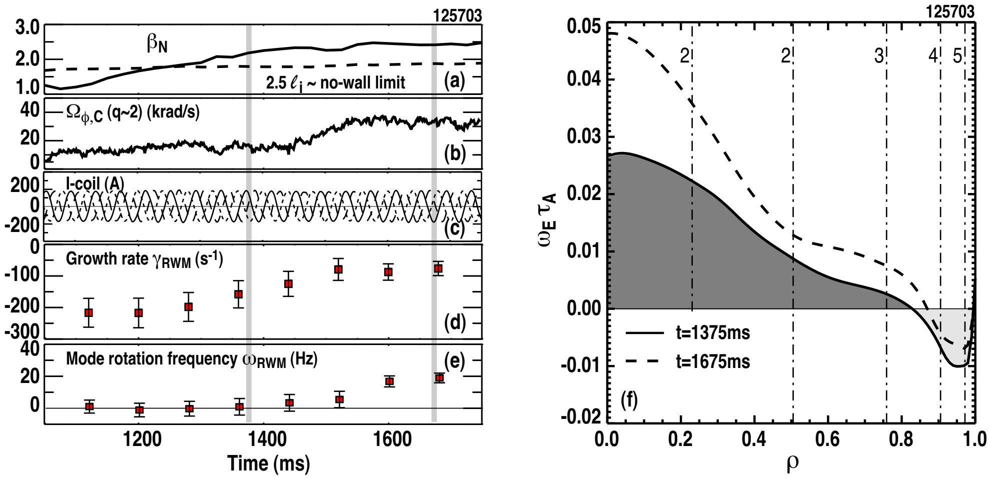


**Figure 4.** Beta (a) and rotation (b) evolution in the wall stabilized discharge 125703, where (c) a low amplitude $n$=1 magnetic field co-rotating with 25 Hz is applied with the I-coil. The measurement of the magnitude and phase of the plasma response yields (d) the (negative) RWM growth rate and (e) the mode rotation frequency. (d) The $\omega_E$ rotation profile at $t$=1375 ms leads to RWM stabilization with a zero frequency RWM.

$\Omega_\phi$ are varied. The (negative) RWM growth rate increases once $\beta$ exceeds the no-wall stability limit, figure 4(d). At the initial low rotation values the mode frequency is virtually zero before it increases with increasing plasma rotation, figure 4(e). This clearly shows that the rotation of the mode with respect to the wall is not necessary for RWM stabilization by plasma rotation, thereby confirming a previous conjecture [17]. The corresponding $\omega_E$ profile, figure 4(f), changes sign at about $\rho$=0.8. Dissipation, which is required to rotate the RWM with respect to the wall, in the central region must be canceled by dissipation with the opposite sign near the edge and stabilization has to occur through a non-dissipative mechanism. A mainly non-dissipative stabilization mechanism is also consistent, firstly, with the weak or non-existent dependence of $\gamma_{\mathrm{RWM}}$ on $\omega_{\mathrm{RWM}}$ observed between $t$=1500 ms and 1700 ms and, secondly, with the low mode rotation of 20 Hz with larger co-rotation observed for $t \geq 1600$ ms, figure 4(b,e).

## 4. Comparison with kinetic modeling

Since the characteristic RWM time scale $\tau_{\mathrm{W}}$ is much longer than most plasma processes the plasma can interact with the perturbation in many ways. Proposed mechanisms include coupling to soundwaves [18], wave-particle resonance of passing ions with the transit frequency $\omega_t$ and of trapped particles with their bounce frequency $\omega_b$ [19] and a resonance of trapped particles at their precession drift frequency $\omega_D$ [20]. In addition to kinetic effects shear Alfvén damping can also contribute to RWM stabilization [21].

The marginally stable profiles obtained in discharges with low NBI torque and good error field correction in co- and counter-rotating plasmas, figure 5(a), are compared to predictions of the soundwave [18] and the semi-kinetic damping model [19] implemented in MARS-F code [22]. Both models assume that $\omega_{\star\mathrm{i}} \ll \Omega$, which is no longer a good approximation for the observed low rotation thresholds (section 2.2). In

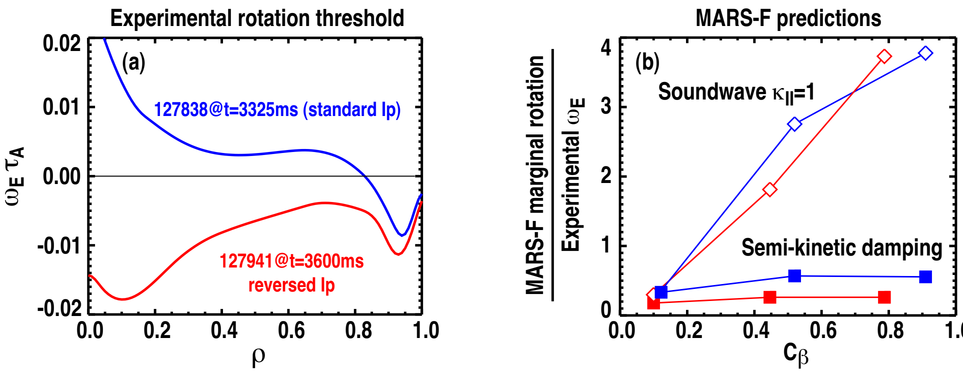


**Figure 5.** Comparison of (a) marginal $\omega_E$ profiles in co- and counter rotating plasmas with (b) MARS-F [22] predictions for the soundwave (diamonds) [18] and the semi-kinetic (sqaures) [19] damping models.

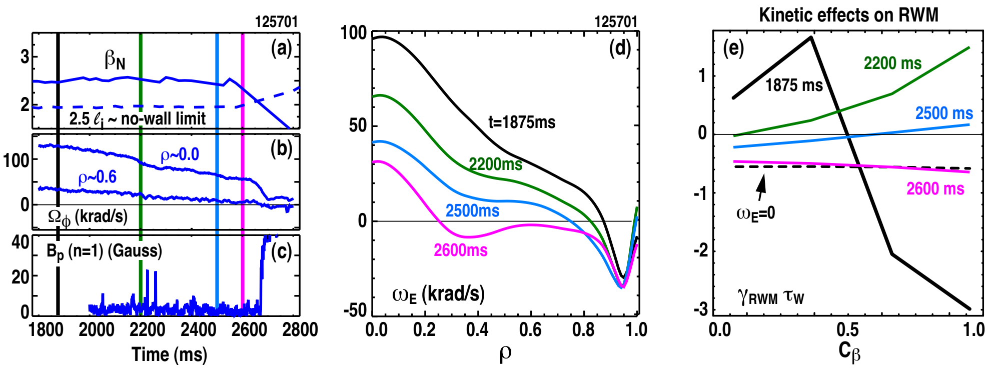


**Figure 6.** In the high beta (a) rotation ramp-down (b) in discharge 125701 the plasma becomes unstable at $t$=2650 ms (c). The stability is analyzed for four $\omega_E$ profiles (d) along the ramp-down and for $\omega_E$=0. The kinetic calculation of the RWM growth rate [23] including the effect of shear Alfvén damping [21] (e) shows a window of instability between high rotation at $t$=1875 ms and low rotation at $t$=2600 ms.

order to address the findings of the comparison of rotation thresholds in co- and counter rotating plasmas, $\omega_E$ is used as the rotation $\Omega$ in the calculations. The experimental pressure profiles are scaled keeping the safety factor profiles constant. The parameter $C_\beta=(\beta-\beta_{\rm nw})/(\beta_{\rm iw}-\beta_{\rm nw})$ describes the gain in $\beta$ between the no-wall and ideal-wall stability limits. In both cases soundwave damping using moderate viscosity $\kappa_{||}$=1 leads to a rotation threshold, which increases with $C_\beta$. At the experimental value of $C_\beta\sim0.4$ the critical rotation clearly exceeds the measured threshold, figure 5(b). The predictions for semi-kinetic damping are generally much lower than the observations, figure 5(b). While the soundwave damping model using $\kappa_{||}$=1 is in disagreement with the experiment, the lower threshold of the semi-kinetic damping model could be reconciled with residual error fields leading to a nonlinear mode onset at an effective rotation threshold above the linear threshold.

The rotation threshold in a similar co-rotating plasma 125701, figure 6(a-c), is also compared to the predictions of a kinetic post-processor to the ideal MHD code

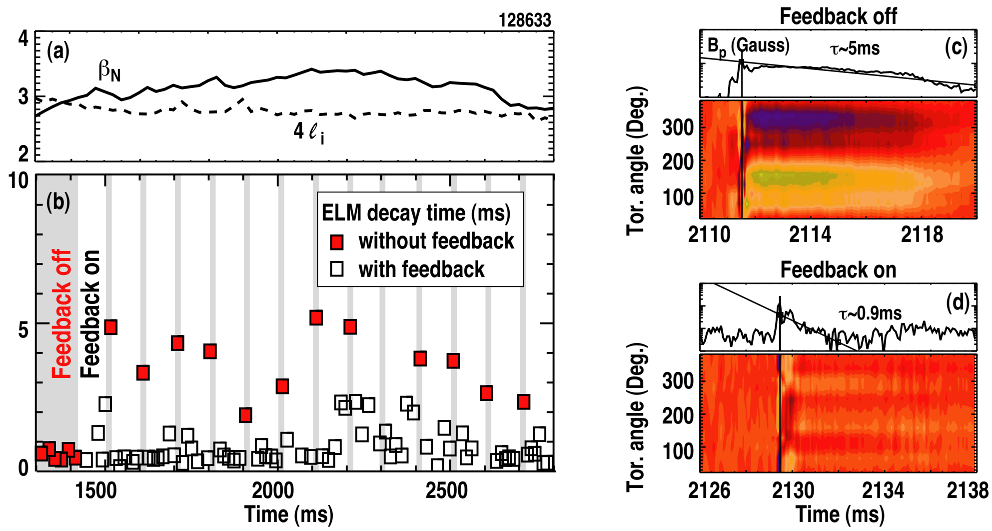


**Figure 7.** In a high $\beta$ advanced tokamak discharge (a) the decay time of the $n$=1 magnetic perturbation following an ELM (b) is decreased by active RWM feedback. While the decay time without feedback is typically 5 ms (c), feedback decreases the decay time below 1 ms (d).

PEST [23]. While these calculations assume the ideal MHD kink mode structure, the kinetic model is more complete taking into account $\omega_D$ and $\omega_{\star i}$. Recently shear Alfvén damping [21] has also been included in the calculation. The stability of the equilibrium at $t$=2500 ms is calculated for rotation profiles at several times throughout the rotation ramp down, figure 6(d,e). The experimental pressure profile is again scaled to span the entire wall stabilized regime. The model predicts stability for the experimental rotation profile at $t$=2500 ms from the no-wall limit ($C_\beta$=0) half way through the wall stabilized regime, which includes the experimental $\beta$. Owing to the resonance with $\omega_D$ the RWM is stabliized across the entire wall-stabilized regime when the rotation decreases further ($t$=2600 ms). A similar stabilizaton is obtained when $\omega_E$ is set to zero figure 6(e) (dashed line). The model, however, does predict instability at intermediate values of rotation ($t$=2200 ms). The effect of shear Alfvén damping is small for the analyzed profiles, but becomes important once the rotation velocity is in the order of a few percent of the Alfvén velocity. Including further stabilizing mechanisms, such as the effect of poloidal rotation, should eventually close the gap to high rotation where shear Alfvén damping is sufficiently strong.

## 5. Feedback

Despite the encouraging observations of wall stabilized discharges with very little momentum input and a stabilization model that extrapolates to zero rotation, one has to realize that the stabilization is weak. The weakly damped RWM can greatly amplify externally applied $n$=1 perturbations of the magnetic field. It has also frequently been observed that plasma generated perturbations such as edge localized modes (ELMs) or fishbones, can be sufficient to trigger a $\beta$ collapse even at high plasma rotation [24].

An active feedback system using a set of 12 control coils inside the DIII-D vacuum vessel accelerates the damping of ELM excited $n$=1 magnetic perturbations in the high $\beta$ advanced tokamak discharge 128633, figure 7(a,b). The decay rate of the perturbation of up to 5 ms without feedback, figure 7(c), is decreased below 1 ms when the feedback is switched on, figure 7(d). This is consistent with the experience that RWM feedback control is essential to reliably access high $\beta$, high performance AT scenarios. [24].

## 6. Summary

DIII-D has demonstrated stable operation above the ideal MHD no-wall stability limit with a greatly reduced NBI torque input and at low plasma rotation. The reduction of $n$=1 magnetic field asymmetries is essential for RWM stability at low rotation. In the presence of $n$=1 field asymmetries the rotation threshold increases, which can be explained by a loss of torque balance leading to a nonlinear RWM onset. Magnetic braking experiments suggest that even the rotation threshold with low NBI torque and good error field correction could be still caused by residual error fields. This is consistent with kinetic predictions of the linear RWM threshold, which can predict stability even without plasma rotation. However, this stabilization is weak and externally applied or internally generated perturbations can lead to an effective rotation threshold well above linear predictions. Active RWM feedback can mitigate the effect of transient perturbations and provide the robustness needed for reliable operation in the wall-stabilized regime.

## Acknowledgments

This work has been supported by the U.S. Department of Energy under DE-FG02-89ER53297, DE-AC02-76CH03073, DE-FC02-04ER54698, and DE-FG02-03ER83657.

## References

[1] Hender T C, Wesley J C *et al* 2007 *Nucl. Fusion* **47** S128
[2] Alper B *et al* 1989 *Plasma Phys. Control. Fusion* **31** 205
[3] Strait E J *et al* 1995 *Phys. Rev. Lett.* **74** 2483
[4] Hender T C *et al* 2004 *Proc. of the 20th IAEA FEC, Villamoura, Portugal* EX/P2-22
[5] Sabbagh A *et al* 2006 *Nucl. Fusion* **46** 635
[6] Garofalo A M *et al* 2002 *Phys. Rev. Lett.* **89** 235001
[7] La Haye R J *et al* 2004 *Nucl. Fusion* **44** 1197
[8] Reimerdes H, Hender T C, Sabbagh S A *et al* 2006 *Phys. Plasmas* **13** 056107
[9] Reimerdes H *et al* 2007 *Phys. Rev. Lett.* **98** 055001
[10] Takechi M *et al* 2007 *Phys. Rev. Lett.* **93** 055002
[11] Strait E J *et al* 2007 *Phys. Plasmas* **14** 056101
[12] Garofalo A M *et al* submitted to *Nucl. Fusion*
[13] Fitzpatrick R 1998 *Phys. Plasmas* **5** 3325
[14] Fitzpatrick R 2002 *Phys. plasmas* **9** 3459
[15] Solomon W M, Burrell K H *et al* 2006 *Phys. Plasmas* **13** 056116
[16] Reimerdes H *et al* 2005 *Nucl. Fusion* **45** 368
[17] Garofalo A M, Jensen T H and Strait E J 2003 *Phys. Plasmas* **10** 4776
[18] Bondeson A and Ward D J 1994 *Phys. Rev. Lett.* **72** 2709
[19] Bondeson A and Chu M S 1996 *Phys. Plasmas* **3** 3013
[20] Hu B and Betti R 2004 *Phys. Rev. Lett.* **93** 105002
[21] Zheng L-J, Kotschenreuther M and Chu M S 2005 *Phys. Rev. Lett.* **95** 255003
[22] Liu Y Q *et al* 2000 *Phys. Plasmas* **7** 3681
[23] Hu B, Betti R and Manickam J 2005 *Phys. Plsmas* **12** 057301
[24] Garofalo A M *et al* 2006 *Phys. Plasmas* **13** 056110